JOURNAL OF SOLID STATE CHEMISTRY 4, 186–194 (1972)

Shear Structure Compounds $(Cr,Fe)_2Ti_{n-2}O_{2n-1}$ derived from the α-PbO_2 Structural Type

I. E. GREY AND A. F. REID

Division of Mineral Chemistry, CSIRO, P.O. Box 124, Port Melbourne, Victoria, 3207, Australia

Received June 16, 1971

Chromium iron titanates, with general formula $(Cr,Fe)_2Ti_{n-2}O_{2n-1}$, $n = 3$, 4, and 5 have been prepared by reacting the component oxides in air at 700–1650°C. The compounds have been characterized by X-ray crystallographic techniques and, where necessary, lattice parameters have been confirmed by selected area electron diffraction. The structures of the compounds are closely related to that of α-PbO_2 and may be derived from it by crystallographic shear parallel to $(110)_{\alpha\text{-}PbO_2}$.

Preliminary results are reported for two series of ordered intergrowth phases, $(M_3O_5)_n(M_4O_7)_m$ and $(M_4O_7)_n(M_5O_9)_m$.

Introduction

In the Cr–Ti–O system, studies by Andersson (*1*) revealed the existence of a number of discrete compounds of general formula $Cr_2Ti_{n-2}O_{2n-1}$, with $n = 6$, 7, 8, and 9, isomorphous with members of the homologous series Ti_nO_{2n-1} (*2*) and V_nO_{2n-1} (*3*). The structures of these compounds are closely related to that of rutile and may be derived from it by crystallographic shear. More recent studies by Flörke (*4*) and by Kwestroo and Roos (*5*) have confirmed the existence of Andersson phases in this system for $n \geqslant 6$. However, the lower homologues in this series, with $n = 3$, 4, and 5, have not been characterized. The composition Cr_2TiO_5, equivalent to $n = 3$, is stabilized in a form isomorphous with V_3O_5 (*6*) by addition of Fe_2TiO_5 or Al_2TiO_5. $Cr_2Ti_2O_7$, $n = 4$, was first identified as a discrete compound, not part of the Andersson phase series, by Hamelin (*7*). Studies to date (*4*) have indicated that it is nonstoichiometric below 1500°C, and has an apparent range of homogeneity. Discussion of this compound has been restricted, because its structure has not been known. No compound has previously been found at the composition $Cr_2Ti_3O_9$, $n = 5$.

In the Fe–Ti–O system, it has been recognized (*8*) that when ilmenite is oxidized at 600–800°C, a phase additional to Fe_2O_3 and TiO_2 is produced. In an examination of this system, we observed that the *d*-spacings of the unknown phase bore a close resemblance to those of $Cr_2Ti_2O_7$. This has prompted a further examination of the Cr_2O_3–Fe_2O_3–TiO_2 system, which has included the determination of the structure of $CrFeTi_2O_7$ from single crystal data (*9*). This last compound proved to be a member of a new homologous series $(Cr,Fe)_2Ti_{n-2}O_{2n-1}$, $n = 3$, 4, 5 whose structures are based on the high pressure form of rutile, (*10–12*) isomorphous with α-PbO_2 (*13*).

We report here the preparation and structural characterization of the members of this series, and of two further series of compounds which are ordered intergrowths of the M_3O_5–M_4O_7 and M_4O_7–M_5O_9 structures, respectively. Both intergrowth series converge to M_4O_7. Their existence provides the basis for the apparent range of homogeneity (*4*) shown by $Cr_2Ti_2O_7$.

Experimental

Preparation of Compounds

Compounds in the Cr_2O_3–Fe_2O_3–TiO_2 phase field were prepared from finely ground, pelletized mixtures of the component oxides, or from preformed $FeTiO_3$. The samples were supported on platinum foil and heated in air at 750–1600°C for periods of 1 day to 1 month, Table I, and then quenched to room temperature. Samples were usually reground at least once after an initial period at the reaction temperature.

Anatase form TiO_2 and Fe_2O_3 were both Fisher Certified Reagents. Reactive, finely divided Cr_2O_3

TABLE I

CHARACTERIZATION OF PHASES IN THE SYSTEM $Fe_2O_3 - Cr_2O_3 - TiO_2$

Starting composition	Temperature °C.	Heating period days	Products[a]
$\underline{M_2O_3 - TiO_2}$			
M = $Fe_{1.0}$	800 to 1400	2	P.B.[b]
$Fe_{0.7}Cr_{0.3}$	1400	2	P.B. + M_3O_5
$Fe_{0.5}Cr_{0.5}$	1250	3	$\underline{M_3O_5}$
	1550	3	$M_3O_5 + M_2O_3$
$Fe_{0.15}Cr_{0.85}$	1400	3	$\underline{M_3O_5}$
	1550	2	$M_3O_5 + (M_3O_5)_n(M_4O_7)_m$
$Fe_{0.1}Cr_{0.9}$	1350	3	$M_3O_5 + M_2O_3$
	1450	2	$M_3O_5 + (M_3O_5)_n(M_4O_7)_m$
$Cr_{1.0}$	1300	3	$M_4O_7 + Cr_2O_3$
	1500	3	$M_4O_7 + Cr_2O_3$
	1550	2	$(M_3O_5)_n(M_4O_7)_m + Cr_2O_3$
$\underline{M_2O_3 - 2TiO_2}$			
M = $Fe_{1.0}$	< 800	30	No reaction
(i) Fe_2O_3	> 800	1	P.B. + TiO_2
(ii) $FeTiO_3$	770	30	$M_5O_9 + Fe_2O_3$
	> 800	1	P.B. + TiO_2
$Fe_{0.9}Cr_{0.1}$	900	4	$M_3O_5 + M_5O_9$
	1150	4	Mainly P.B. + TiO_2
$Fe_{0.75}Cr_{0.25}$	900	4	$M_3O_5 + M_5O_9$
	1200	2	$\underline{M_4O_7}$
	1350	2	M_4O_7 + P.B. + TiO_2
$Fe_{0.5}Cr_{0.5}$	1400	4	$\underline{M_4O_7}$
	1500	4	$\underline{M_4O_7}$ (single crystals)
$Fe_{0.2}Cr_{0.8}$	900	2	$(M_4O_7)_n(M_5O_9)_m + M_2O_3$
	1500	2	$\underline{M_4O_7}$
$Cr_{1.0}$	1100	2	A.P.[c] + Cr_2O_3
	1200	2	M_5O_9 + A.P. + Cr_2O_3
	1350	2	$(M_4O_7)_n(M_5O_9)_m$
	1650	2	$\underline{M_4O_7}$
$\underline{M_2O_3 - 3TiO_2}$			
M = $Fe_{1.0}$	< 800	30	Incomplete reaction
	> 800	2	P.B. + TiO_2
$Fe_{0.9}Cr_{0.1}$	900	1	P.B. + TiO_2
$Fe_{0.7}Cr_{0.3}$	1050	3	$\underline{M_5O_9}$
	1200	3	$\underline{M_5O_9}$
$Fe_{0.5}Cr_{0.5}$	1100	3	$\underline{M_5O_9}$
	1250	2	$\underline{M_5O_9}$
	1500	2	$(M_4O_7)_n(M_5O_9)_m$
$Fe_{0.15}Cr_{0.85}$	1250	3	$\underline{M_5O_9}$ + A.P. (trace)
	1550	3	$(M_4O_7)_n(M_5O_9)_m$ + A.P.
$Cr_{1.0}$	1200	2	A.P.
	1400	2	$(M_4O_7)_n(M_5O_9)_m$ + A.P.
	1600	1	$(M_4O_7)_n(M_5O_9)_m$ + A.P.
$\underline{2M_2O_3 - 5TiO_2}$			
$Fe_{0.2}Cr_{0.8}$	1400	3	$(M_4O_7).(M_5O_9)$
$\underline{3M_2O_3 - TiO_2}$			
$Fe_{0.2}Cr_{0.8}$	1500	3	$(M_3O_5)_2.(M_4O_7)$

a. Identified from X-ray powder diffractograms

b. P.B. : Pseudobrookite

c. A.P. : Rutile based Andersson Phases.

was prepared by thermal decomposition of analytical grade ammonium dichromate, heated at a final temperature of 900°C for 30 min. The $FeTiO_3$ was prepared by reduction at 900°C of a pelleted mixture of $Fe_2O_3:2TiO_2$ in a gas flow of composition 60% H_2:40% H_2O.

X-Ray Diffraction

X-Ray powder patterns were obtained with a Philips diffractometer fitted with a graphite monochromator, using Cu*Kα* radiation. Potassium chloride, $a_0 = 6.2931$, was used as an internal standard for lattice parameter determination, and slow scan rates were used to ensure high precision in the data.

Results

Characterization of Phases

The product phases listed in Table I were characterized by their X-ray powder patterns, Fig. 1 and Table II. In each case, the indexing of the patterns was checked by least squares refinement of the lattice parameters, using precise data obtained with KCl as an internal standard. In several cases the unit cell was also verified from selected area electron diffraction patterns (*14*). The identification of the phases in the Cr_2O_3–Fe_2O_3–TiO_2 system was greatly facilitated by having completely indexed powder patterns based on single crystal data for $(Cr, Fe)_2TiO_5$ with the V_3O_5 structure (*6*) and for

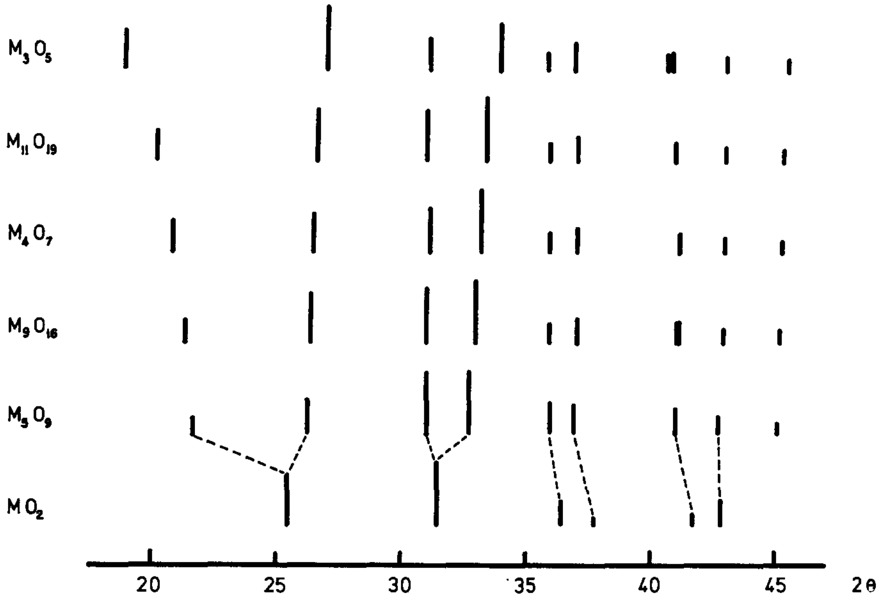

FIG. 1. Powder diffraction data for chromium iron titanate shear structure compounds. Intensities are to scale.

$M_3O_5 = (Cr_{0.5}Fe_{0.5})_2TiO_5$, $M_{11}O_{19} \equiv (M_3O_5)\cdot(M_4O_7)_2 = (Cr_{0.8}Fe_{0.2})_6Ti_5O_{19}$,
$M_4O_7 = Cr_2Ti_2O_7$, $M_9O_{16} \equiv M_4O_7\cdot M_5O_9 = (Cr_{0.8}Fe_{0.2})_4Ti_5O_{16}$
MO_2 = high-pressure form of TiO_2 (*11*), with the α-PbO_2 structure.

$CrFeTi_2O_7$, for which the structure was determined in a companion study (*9*). These two structures were recognized as being those of the lower homologues of a series M_nO_{2n-1} related to the high pressure, or α-PbO_2 form of TiO_2 as discussed below. As illustrated in Fig. 1, the powder patterns of the compounds in the series show a marked similarity towards one another, and to the pattern of the α-PbO_2 form of TiO_2 to which they should converge as *n* increases.

Phases produced from $M_2O_3\cdot TiO_2$ Compositions, M = Cr, Fe

The compound Fe_2TiO_5 has the pseudobrookite structure (*15*). According to Kwestroo and Roos (*5*), up to 15% of Fe can be replaced by Cr without change of structure, and we obtained a similar result. For higher Cr contents we found that there exists a two-phase region comprising pseudobrookite and V_3O_5 structure types, up to about 50 mole% of Cr. At 50 mole%, the composition $FeCrTiO_5$ formed a single phase of V_3O_5-type at 1250°C. At higher temperatures, M_2O_3, close to Fe_2O_3 in composition, was lost from the structure as a second phase. However, the powder pattern of the remaining phase could still be indexed precisely on the basis of a V_3O_5-type cell, indicating a real range of homogeneity for this structure (see Tables II and III).

As the Cr content was increased from 50 to 85 mole%, the V_3O_5 structural type could still be obtained, in agreement with Kwestroo and Roos. However, at temperatures above 1450°C new phases appeared for which the powder patterns were intermediate between those for M_3O_5 and M_4O_7. These patterns could be satisfactorily indexed on the basis that they were ordered intergrowths of M_3O_5 and M_4O_7. In separate preparations, compositions $(M_3O_5)_n(M_4O_7)_m$ were prepared as single phases and, in several cases, the unit cell parameters have been confirmed from electron diffraction patterns of single crystal fragments. The X-ray diffraction data for a typical intergrowth phase, $(M_3O_5)\cdot(M_4O_7)_2$ is given in Fig. 1 and Table II. These interesting compounds will be reported in detail elsewhere (*14*).

Phases produced from $M_2O_3{:}2TiO_2$ Compositions and by the Oxidation of Ilmenite

Reaction of $Fe_2O_3{:}2TiO_2$ mixtures gave only pseudobrookite plus rutile, the reaction being very slow below 800°C. Haggerty and Lindsley (*16*) have shown by hydrothermal studies that pseudobrookite forms above 585°C, but below that temperature it is

TABLE II

X-RAY POWDER DIFFRACTION DATA[a] FOR CHROMIUM IRON TITANATE SHEAR STRUCTURE COMPOUNDS BASED ON THE α-PbO_2 TYPE

1. $(Cr_{0.50}Fe_{0.50})_2TiO_5$ (1250°C)

h	k	l	$\sin^2\theta_{calcd.}$	$\sin^2\theta_{obsd.}$
0	0	2	0.02703	0.02705
0	1	1	0.03036	0.03040
-2	0	2	0.05490	0.05480
-2	1	1	0.07218	0.07210
0	1	3	0.08443	0.08445
0	2	0	0.09443	0.09462
-2	1	3	0.09836	0.09855
2	1	1	0.10007	0.10016
-2	0	4	0.10812	0.10830
-1	2	2	0.12147	0.12165
-3	1	1	0.13490	0.13492
-2	2	2	0.14933	0.14936
0	1	5	0.19256	0.19251
-2	2	4	0.20255	0.20252
2	0	4	0.21967	0.21940
-4	1	3	0.22382	0.22374
0	0	6	0.24331	0.24315
-2	3	1	0.26103	0.26111
0	3	3	0.27329	0.27355
2	3	1	0.28892	0.28917

2. $(Cr_{0.50}Fe_{0.50})_2TiO_5$ (1550°C)

h	k	l	$\sin^2\theta_{calcd.}$	$\sin^2\theta_{obsd.}$
0	0	2	0.02694	0.02685
0	1	1	0.03033	0.03025
-2	0	2	0.05471	0.05472
-2	1	1	0.07201	0.07203
0	1	3	0.08421	0.08421
0	2	0	0.09437	0.09443
2	1	1	0.09985	0.10005
-2	0	4	0.10769	0.10756
-1	2	2	0.12129	0.12122
-3	1	1	0.13455	0.13468
-2	2	2	0.14908	0.14911
0	1	5	0.19198	0.19203
-2	2	4	0.20207	0.20224
2	0	4	0.21904	0.21910
-4	1	3	0.22310	0.22310
-2	3	1	0.26075	0.26088
0	3	3	0.27295	0.27300
2	3	1	0.28858	0.28853
4	0	2	0.30501	0.30488

3. $Cr_2Ti_2O_7$ (1650°C)

h	k	l	$\sin^2\theta_{calcd.}$	$\sin^2\theta_{obsd.}$
0	0	3	0.03280	0.03271
0	1	2	0.03847	-
-2	0	3	0.05304	0.05285
-2	1	2	0.07213	0.07234
0	1	4	0.08220	0.08212
0	2	0	0.09556	0.09570
-2	1	4	0.09702	-
2	1	1	0.10144	0.10142
-2	0	6	0.11119	0.11139
-1	2	3	0.12340	0.12360
-3	1	2	0.13432	0.13432
-2	2	3	0.14860	0.14855
0	1	7	0.20248	0.20252
-2	2	6	0.20675	0.20660
2	0	5	0.21870	0.21880
-4	1	5	0.22280	0.22280
0	0	8	0.23330	0.23370
-2	3	2	0.26325	0.26326
0	3	4	0.27332	0.27324
2	3	1	0.29257	0.29257

4. $Fe_2Ti_3O_9$ (770°C)

h	k	l	$\sin^2\theta_{calcd.}$	$\sin^2\theta_{obsd.}$
0	0	4	0.03532	0.03527
0	1	3	0.04367	-
-2	0	4	0.05167	0.05187
-2	1	3	0.07163	0.07168
0	1	5	0.07900	0.07915
0	2	0	0.09521	0.09518
2	1	1	0.10045	0.10026
-2	0	8	0.11115	0.11093
-1	2	4	0.12299	0.12293
-3	1	3	0.13274	0.13284
-2	2	4	0.14690	0.14706
0	1	9	0.20262	0.20273
-2	2	8	0.20636	0.20625
2	0	6	0.21201	0.21220
-4	1	7	0.22059	0.22062
-2	3	3	0.26205	0.26219
0	3	5	0.26941	0.26951
2	3	1	0.29087	0.29067

5. $(Cr_{0.80}Fe_{0.20})_6Ti_5O_{19}$ (1500°C)

h	k	l	$\sin^2\theta_{calcd.}$	$\sin^2\theta_{obsd.}$
0	0	8	0.03112	0.03103
0	1	5	0.3595	-
-2	0	8	0.05341	0.05332
-2	1	5	0.07200	0.07190
0	1	11	0.08263	0.08271
0	2	0	0.09515	0.09515
-2	1	11	0.09115	-
2	1	3	0.10093	0.10094
-2	0	16	0.11007	0.11013
-1	2	8	0.12267	0.12264
-3	1	5	0.13428	0.13450
-2	2	8	0.14857	0.14861
0	1	19	0.19934	0.19930
-2	2	16	0.20523	0.20526
2	0	14	0.21854	0.21874
-4	1	13	0.22267	0.22258
0	0	22	0.23534	0.23540
-2	3	5	0.26232	0.26234
0	3	11	0.27295	0.27300
2	3	3	0.29124	0.29115

6. $(Cr_{0.80}Fe_{0.20})_4Ti_5O_{16}$ (1450°C)

h	k	l	$\sin^2\theta_{calcd.}$	$\sin^2\theta_{obsd.}$
0	0	7	0.03442	0.03450
0	1	5	0.04145	-
-2	0	7	0.05239	0.05235
-2	1	5	0.07205	0.07227
0	1	9	0.08080	0.08080
0	2	0	0.09558	0.09570
2	1	2	0.10146	0.10137
-2	0	14	0.11150	0.11143
-1	2	7	0.12345	0.12356
-3	1	5	0.13394	0.13408
-2	2	7	0.14797	0.14793
0	1	16	0.20374	0.20350
-2	2	14	0.20708	0.20703
2	0	11	0.21654	0.21680
-4	1	12	0.22217	0.22214
-2	3	5	0.26319	0.26349
0	3	9	0.27196	0.27199
2	3	2	0.29262	0.29257

[a] $CuK\alpha_1$ radiation, KCl internal standard, a = 6.2931 Å

unstable with respect to the oxides. However, when finely powdered ilmenite, also with an Fe:Ti ratio of 1:1, was heated in air at temperatures below 800°C, a new iron titanate formed. Prolonged heating at 770°C gave the new phase together with exsolved Fe_2O_3. The weight per cent of Fe_2O_3 was

TABLE III

LATTICE PARAMETERS OBSERVED[a] AND CALCULATED FOR SHEAR STRUCTURE COMPOUNDS BASED ON THE α-PbO_2 TYPE

Phase		a Å	b Å	c Å	β°	Volume Å^3
$(Cr_{0.50}Fe_{0.50})_2TiO_5$	(1250°C)[b]	6.990 (2)[c]	5.013 (2)	10.039 (4)	111.05 (4)	328.31
	(1550°C)	7.001 (3)	5.001 (2)	10.058 (4)	111.07 (4)	328.63
$(Cr_{0.85}Fe_{0.15})_2TiO_5$	(1350°C)	7.004 (3)	5.000 (2)	9.964 (4)	111.29 (4)	325.14
	(1500°C)	6.998 (3)	5.007 (2)	9.980 (4)	111.24 (4)	325.94
Calculated[d] for M_3O_5		7.10	4.91	9.46	112.9	303.8
$(Cr_{0.50}Fe_{0.50})_2Ti_2O_7$		7.032 (3)	5.000 (2)	14.425 (6)	116.59 (4)	453.56
$Cr_2Ti_2O_7$		7.021 (3)	4.983 (2)	14.301 (6)	116.86 (4)	446.35
Calculated for M_4O_7		7.10	4.91	13.86	118.3	425.44
$(Cr_{0.85}Fe_{0.15})_2Ti_3O_9$		7.031 (3)	4.974 (2)	18.788 (9)	119.72 (4)	570.78
$Fe_2Ti_3O_9$		7.071 (4)	4.997 (3)	18.862 (10)	119.56 (5)	579.69
Calculated for M_5O_9		7.10	4.91	18.32	121.1	546.9
$(Cr_{0.80}Fe_{0.20})_4Ti_5O_{16}$		7.034 (3)	4.983 (2)	33.074 (15)	118.52 (4)	1018.5
Calculated[e] for $(M_4O_7).(M_5O_9)$		7.10	4.91	32.16	120.0	970.9
$(Cr_{0.80}Fe_{0.20})_6Ti_5O_{19}$		7.019 (3)	4.994 (2)	38.654 (18)	115.36 (4)	1224.3
Calculated[e] for $2(M_4O_7).(M_3O_5)$		7.10	4.91	37.15	116.9	1155.0

a. From least squares refinement of the diffraction data

b. Temperature of preparation

c. The numbers in parentheses after numerical values are the standard deviations in the last figure shown

d. Calculated values from vectorial expressions given in text

e. Calculated by vector combination of end member cells (from d).

determined by quantitative X-ray peak area analysis (*17*), and the ratio of Fe_2O_3 to TiO_2 in the new phase was deduced to be 1:3, based on an observed value of 1:2.8 ± 0.3. The X-ray powder pattern, Table II, could be indexed completely on the basis of this compound being homologous with $(Cr,Fe)_2TiO_5$ and $(Cr,Fe)_2Ti_2O_7$, i.e., corresponding to $n = 5$ in the homologous series $(Cr,Fe)_2Ti_{n-2}O_{2n-1}$. Its formation from ilmenite thus corresponds to the reaction:

$$6FeTiO_3 + 3O = 2Fe_2Ti_3O_9 + Fe_2O_3.$$

Above 800°C, $Fe_2Ti_3O_9$ decomposed to pseudobrookite plus rutile.

Reaction of compositions $M_2O_3 \cdot 2TiO_2$ in which up to 30 mole% of Fe was replaced by Cr gave mixtures of M_3O_5 and M_5O_9. Above 30% replacement, single phase compounds $(Cr,Fe)_2Ti_2O_7$ were obtained, and heating of the composition $FeCrTi_2O_7$ at 1500°C for several days gave single crystals suitable for X-ray structure analysis (*9*).

With increasing chromium contents, the temperatures of formation of single phase M_4O_7 were progressively increased. Temperatures of ~1550°C or higher were required to form single phase $Cr_2Ti_2O_7$ in accordance with the results reported by Flörke (*4*). Heating $Cr_2Ti_2O_7$ at a series of temperatures below 1550°C produced mixtures containing rutile-based Andersson phases together with new phases, whose powder patterns were intermediate between those of the M_4O_7 and M_5O_9 structures based on α-PbO_2 type. As with the M_3O_5–M_4O_7 intergrowths, several chromium–iron members of the intergrowth series could be prepared as pure phases by reacting appropriate starting compositions. The indexed powder pattern for a 1:1 intergrowth, $(Cr,Fe)_4Ti_5O_{16}$, is given in Table II. The lattice parameters, Table III, were confirmed by electron diffraction (*14*).

Phases produced from M_2O_3:$3TiO_2$ Composition

$Fe_2Ti_3O_9$ could not be produced by the reaction of Fe_2O_3 with $3TiO_2$, but was prepared by the oxidation of ilmenite, (section above). The formation of this compound appears to depend on divalent iron as an intermediate species, and it could also be formed by heating in air mixtures of metallic iron, Fe_2O_3 and TiO_2. This behavior most probably reflects the metastable nature of the compound, and the need to provide a specific reaction path for its formation. Above 800°C, $Fe_2Ti_3O_9$ decomposes to Fe_2TiO_5 (pseudobrookite) plus rutile. We found that hydrothermal treatment of $Fe_2Ti_3O_9$ at 500°C and 0.5 kbar led to disproportionation to Fe_2O_3 plus TiO_2 as also observed for pseudobrookite (*16*).

Mixed iron chromium titanates with the composition $(Fe,Cr)_2Ti_3O_9$ were difficult to prepare as pure equilibrium single-phase materials. There is a delicate balance between iron:chromium content and the narrow temperature range over which single-phase M_5O_9 may be obtained. If the temperatures were too high, intergrowth phases $(M_4O_7)_n(M_5O_9)_m$ were formed, and invariably the products were contaminated by small amounts of Andersson phases. However, from predominantly single-phase M_5O_9 preparations, single-crystal electron diffraction patterns were obtained, which confirmed the unit cell given in Table III.

Discussion

The compounds $(Cr_xFe_{1-x})_2TiO_5, 0.85 \geq x \geq 0.50$ are isomorphous with V_3O_5, as shown by Kwestroo and Roos (*5*) and confirmed in this work. The structure of V_3O_5 may be derived from that of rutile by crystallographic shear parallel to $(1\bar{2}1)$ rutile, although this has not generally been recognized (*18*). The structure is, therefore, the lowest member of the homologous series of Andersson phases V_nO_{2n-1} (*3*), although these are triclinic where V_3O_5 is monoclinic.

The V_3O_5 structure type may alternatively, and more simply, be considered to derive from the application of crystallographic shear to the α-PbO_2 type structure. These two structures have a common 5 Å unit cell edge, corresponding to $\bar{a}+\bar{b}$ in a

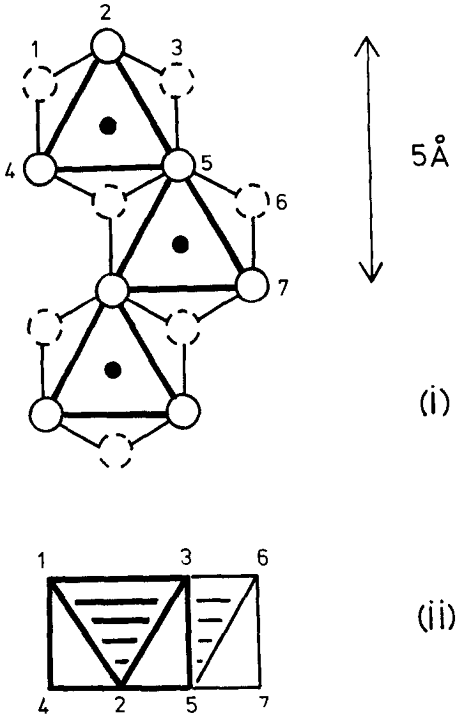

FIG. 2. Representation of structural elements based on hexagonal close packing of oxygen. Part (i) shows a chain of edge-sharing octahedra as in the α-PbO_2 type structure. Heavily drawn circles represent oxygen atoms above the plane, dashed circles oxygens below the plane, and black circles metal atoms in the plane of the paper. The 5 Å axis, $\bar{a}+\bar{b}$ for hexagonally close packed oxygen layers, is shown. (ii) An idealized representation of the chains of edge-shared octahedra of Part (i) as viewed down the 5 Å axis. The correspondence between the two views is shown by the numbering of relevant oxygen atoms 1–7. Andersson and Galy (*19*) have shown how this representation is readily extended to include face and corner sharing.

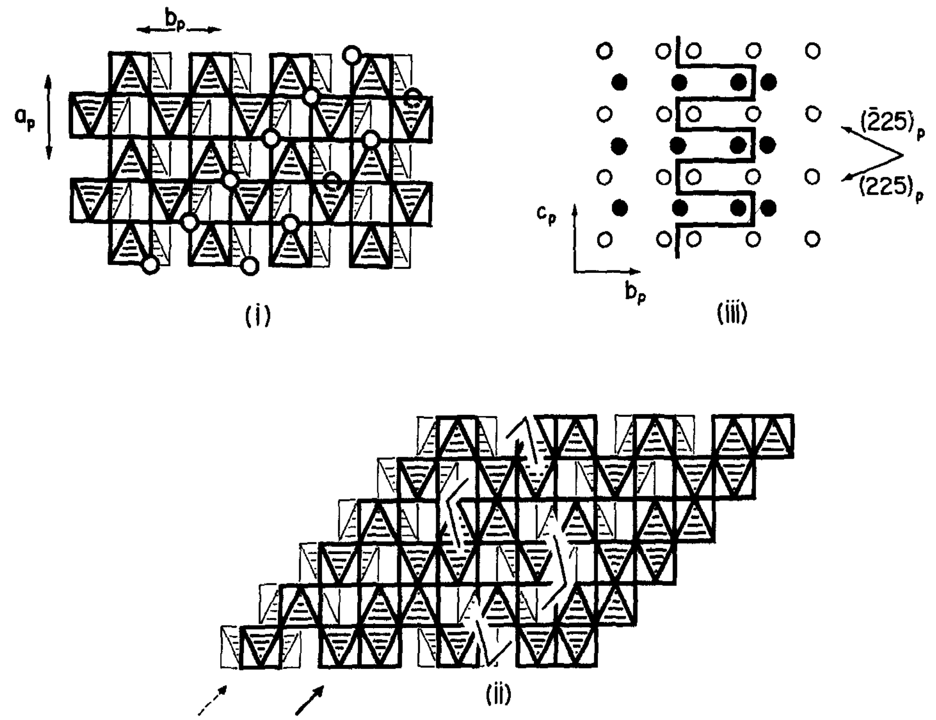

FIG. 3. (i) α-PbO_2 structure. Circles represent the oxygen sites eliminated in producing a $[110]_{\alpha\text{-}PbO_2}$ step shear [as in $(Cr,Fe)_2Ti_{n-2}O_{2n-1}$]. Subscript p refers to α-PbO_2. (ii) $(Cr,Fe)_2TiO_5$ structural type, isostructural with V_3O_5 (*6*). The direction of the shear plane is shown by the arrows. (iii) (110) step shear in the α-PbO_2 type structure, viewed down $[100]_{\alpha\text{-}PbO_2}$; open circles represent metal atoms at $z = \frac{1}{4}$ and full circles represent metal atoms at $z = \frac{3}{4}$. The shear elements lie on intersecting planes parallel to $(225)_{\alpha\text{-}PbO_2}$ and $(\bar{2}25)_{\alpha\text{-}PbO_2}$.

hexagonally close packed arrangement of oxygen atoms, Fig. 2. The relationships between them may be, therefore, illustrated in two-dimensional projections down the 5 Å axes, Figs. 2 and 3.

The following discussion relates to a convenient way of describing the relationship of the shear structure for V_3O_5 and the homologous $(Cr,Fe)_2Ti_{n-2}O_{2n-1}$ compounds to the structure of the α-PbO_2 type. It is not meant to imply that the actual mechanism for formation of the shear planes proceeds in this way.

To form the V_3O_5 structural type from that of α-PbO_2 by crystallographic shear, we consider the initial formation of ordered oxygen vacancies as shown in Fig. 3(i). Application of the shear vector $\frac{1}{4}[010]_{\alpha\text{-}PbO_2}$ to reform octahedral coordination about each metal atom results in the formation of a "step shear" parallel to $[110]_{\alpha\text{-}PbO_2}$. In Fig. 3(iii) the step shear is viewed down $[100]_{\alpha\text{-}PbO_2}$. It is seen that the shear interface is "stepped", being displaced by $5/4[010]_{\alpha\text{-}PbO_2}$ between alternate layers of metal atoms along $[001]_{\alpha\text{-}PbO_2}$.

In Fig. 4 is shown a perspective view down $[1\bar{1}0]_{\alpha\text{-}PbO_2}$ of a section of the α-PbO_2 type structure after the application of a step shear of the type described above. It is seen that shearing of the α-PbO_2 structure results in a reforming of the "zig-zag" strings to give linear rutile-like strings, three octahedra in length. In effect the α-PbO_2 structural type, unstable at atmospheric pressure, is stabilized by a partial collapse of the structure to give rutile-like blocks.

The structures of the members of the homologous series $(Cr,Fe)_2Ti_{n-2}O_{2n-1}$ may be derived from that of α-PbO_2 by application of this step shear at regular intervals, the separation between shear planes increasing with n. The structure of $(Cr,Fe)_2TiO_5$, isomorphous with V_3O_5, $n = 3$, is shown in Fig. 3(ii) while that of $(Cr,Fe)_2Ti_2O_7$, $n = 4$, and the inferred structure of $(Cr,Fe)_2Ti_3O_9$, $n = 5$, are represented in Fig. 5.

The unit cell parameters for the "ideal" M_nO_{2n-1} homologues are simply related to those for the α-PbO_2 structural type by the following vectorial expressions.

$$\tilde{a} = -\tilde{a}_{\alpha\text{-}PbO_2} + \tilde{b}_{\alpha\text{-}PbO_2},$$

$$\tilde{b} = \tilde{c}_{\alpha\text{-}PbO_2},$$

$$\tilde{c} = (n-1)\,\tilde{a}_{\alpha\text{-}PbO_2} + (\tilde{b}/2)_{\alpha\text{-}PbO_2}.$$

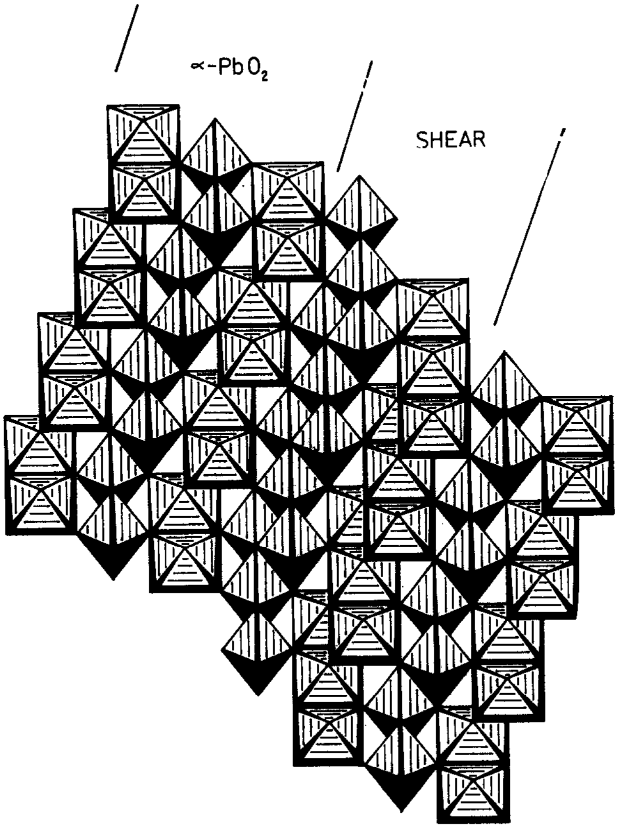

FIG. 4. The α-PbO_2 structure, after application of a $(110)_{\alpha\text{-}PbO_2}$ step shear. The structure is viewed down $[1\bar{1}0]_{\alpha\text{-}PbO_2}$.

Idealized parameters have been calculated using unit cell parameters of McQueen et al. for the high-pressure form of TiO_2 (*11*). They are compared with the observed values for representative homologues in Table III. The unit cell parameters given for M_3O_5 are simply related to those previously chosen (*6*) for V_3O_5 by the vector expressions:

$$\bar{a} = \bar{a}_{V_3O_5} + \bar{c}_{V_3O_5}, \quad \bar{b} = \bar{b}_{V_3O_5}, \quad \bar{c} = -\bar{a}_{V_3O_5},$$

and enable the structural comparisons more easily to be made.

The agreement between the calculated and observed unit cell parameters is reasonable, with a deviation not exceeding 2% for the *a* and *b* parameters and the monoclinic angle. The agreement is not so good for the *c* parameter which effectively defines the shear plane separation; in each case the calculated parameter is smaller than that observed. A similar observation was made by Andersson for the corresponding rutile-based M_nO_{2n-1} homologues and may be accounted for by the expansion of the real structures due to repulsion between the metal atoms in the face shared octahedra.

In the delineation of the phase fields in the Cr_2O_3–Fe_2O_3–TiO_2 system, it was evident that formation of the M_nO_{2n-1} phases based on α-PbO_2 shear was markedly dependent on the Cr:Fe ratio. Neither pure Cr_2TiO_5 nor pure Fe_2TiO_5 form this type of structure, but the composition range $(Cr_xFe_{1-x})_2TiO_5$, $0.85 \geqslant x \geqslant 0.50$, is isomorphous with V_3O_5. Although $Cr_2Ti_2O_7$ is a stable, congruently melting compound, the corresponding $Fe_2Ti_2O_7$ end member has not been made and Cr, Fe compositions isomorphous with $Cr_2Ti_2O_7$ are obtained only with chromium contents greater than 30 mole%. Formation of $(Cr,Fe)_2Ti_3O_9$ is favored by high iron, low chromium contents. This behavior appears to be related to the electronic configurations and consequent cooperative spin-ordering properties of the end member oxides Cr_2O_3 and Fe_2O_3, and is certainly not a simple consequence of ionic size.

In the $(Cr,Fe)_2Ti_{n-2}O_{2n-1}$ series, we were unable to obtain homologues with $n > 5$ and $n = 5$ appears to correspond to the maximum size of the slabs of α-PbO_2 type structure which may be stabilized in this system at atmospheric pressure. However,

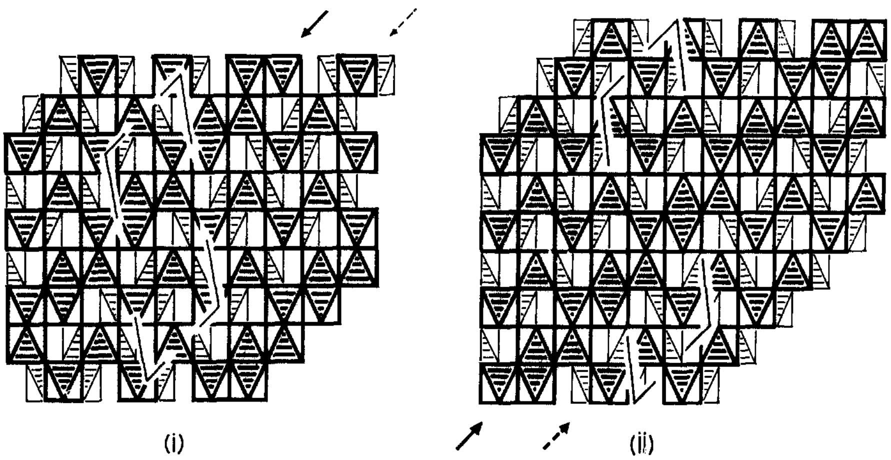

FIG. 5. (i) Representation of the structure of $(Cr,Fe)_2Ti_2O_7$ as found for $(Cr_{0.5}Fe_{0.5})_2Ti_2O_7$ (9). (ii) The inferred structure of $(Cr,Fe)_2Ti_3O_9$. The direction of the shear planes are shown by the arrows.

partial replacement of titanium with zirconium simulates high pressures, and we have been able to obtain homologues $(Cr,Fe)_2(Ti,Zr)_{n-2}O_{2n-1}$ with $n > 5$, as well as new intergrowth phases. The general structural principles outlined here for the lower homologues of the series $(Cr,Fe)_2Ti_{n-2}O_{2n-1}$ will be extended in a later publication to describe the more complicated cases of the intergrowth phases.

Acknowledgments

The authors express their gratitude to Dr. J. G. Allpress for assistance in confirming the unit cell parameters by electron diffraction and to Dr. W. G. Mumme for helpful discussions.

References

1. S. ANDERSSON, A. SUNDHOLM, AND A. MAGNELI, *Acta Chem. Scand.* **13,** 989 (1959).
2. S. ANDERSSON, B. COLLEN, U. KUYLENSTIERNA, AND A. MAGNELI, *Acta Chem. Scand.* **11,** 1641 (1957).
3. G. ANDERSSON, *Acta Chem. Scand.* **8,** 1599 (1954).
4. O. W. FLORKE AND C. W. LEE, *J. Solid State Chem.* **1,** 445 (1970).
5. W. KWESTROO AND A. ROOS, *J. Inorg. Nucl. Chem.* **13,** 325 (1960).
6. S. ASBRINK, S. FRIBERG, A. MAGNELI, AND G. ANDERSSON, *Acta Chem. Scand.* **13,** 603 (1959).
7. M. HAMELIN, *Bull. Soc. Chim. Fr.* **1957,** 1421.
8. M. D. KARKHANAVALA AND A. C. MOMIN, *Econ. Geol.* **54,** 1095 (1959).
9. I. E. GREY AND W. G. MUMME, unpublished results.
10. N. A. BENDELLIANY, S. V. POPOVA, AND L. F. VERESHCHAGIN, *Geokhimiya* **1966,** 499.
11. R. G. MCQUEEN, J. C. JAMIESON, AND S. P. MARSH, *Science* **155,** 1404 (1967).
12. P. Y. SIMONS AND F. DACHILLE, *Acta Crystallogr.* **23,** 334 (1967).
13. A. I. ZASLEVSKIJ AND S. S. TOLKACEV, *Zh. Fiz. Khim.* **26,** 743 (1952).
14. J. ALLPRESS, I. E. GREY, AND A. F. REID, unpublished results.
15. L. PAULING, *Z. Kristallogr, Kristallgeometrie, Kristallphys, Kristallchem* **73,** 97 (1930).
16. S. E. HAGGERTY AND D. H. LINDSLEY, *Carnegie Inst. Washington Yearb* **68,** 247 (1970).
17. G. M. FAULRING AND K. D. CARPENTER, *in* "Advances in X-Ray Analysis," (W. M. Mueller, ed.) Vol. 1, p. 59. Plenum Press, NY (1960).
18. B. G. HYDE, private communication.
19. S. ANDERSSON AND J. GALY, *J. Solid State Chem.* **1,** 576 (1970).